Journal of Medicinal Chemistry

ARTICLE

pubs.acs.org/jmc

In Vitro and In Vivo Antitumor Activities and DNA Binding Mode of Five Coordinated Cyclometalated Organoplatinum(II) Complexes Containing Biphosphine Ligands

Michael Frezza,[†] Q. Ping Dou,*[,†] Yan Xiao,[†] Hamidreza Samouei,[‡] Mehdi Rashidi,*[,‡] Fayezeh Samari,[‡] and Bahram Hemmateenejad*[,‡]

[†]The Developmental Therapeutics Program, Barbara Ann Karmanos Cancer Institute, and Departments of Oncology, Pharmacology and Pathology, School of Medicine, Wayne State University, 540.1 HWCRC, 4100 John R Road, Detroit, Michigan United States

[‡]Chemistry Department, College of Sciences, Shiraz University, Shiraz 71454, Iran

ABSTRACT: New complexes [Pt(C^N)Cl(dppa)] (**1**), and [Pt(C^N)Cl(dppm)] (**2**), (C^N. deprotonated 2-phenylpyridine; dppa. bis(diphenylphosphino)amine; dppm. bis(diphenylphosphino)methane) were suggested to have pentacoordinated geometry as investigated by NMR and conductometry. Pharmacological effects of **1** and **2** were evaluated for their proteasome-inhibitory and apoptosis-inducing activities under in vitro and in vivo conditions, showing significant proteasome-inhibitory activity against purified 20S proteasome, while **2** demonstrated superior inhibitory activity against cellular 26S proteasome. Consistently, this effect was associated with higher levels of proteasome target proteins and apoptosis induction in breast cancer cells. Importantly, preliminary studies show **1** and **2** were able to exert a similar effect in vivo by inhibiting the growth of breast cancer xenografts in mice, which was associated with proteasome inhibition and apoptosis induction. Interaction of **1** and **2** with herring sperm DNA was investigated by fluorimeteric emission, suggesting that Pt^{II}-containing biphosphine complexes with DNA binding capabilities can also target and inhibit the tumor proteasome.

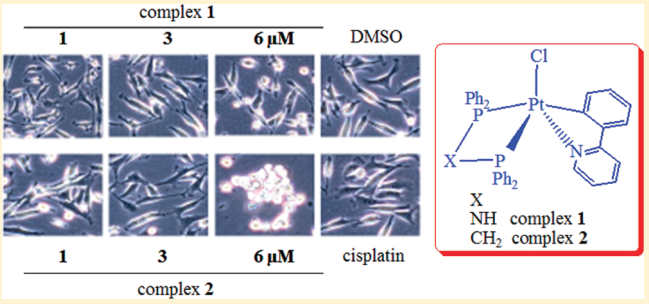

INTRODUCTION

Since the landmark discovery of the antitumor activity of *cis*-diamminedichloroplatinum(II), *cis*-[$Pt(NH_3)_2Cl_2$] (cisplatin),[1] many other Pt complexes have been designed, synthesized, and tested in order to circumvent the cisplatin acquired resistance, side effects, toxicity, and low water solubility in an effort to increase the efficacy of the drug.[2] The proposed mechanism of action of these anticancer agents have yet to be completely understood, but it is believed that the formation of bonds between the platinum center and DNA leading to the formation of coordinative cross-links is responsible for the cytotoxicity of cisplatin.[3] Additionally, platinum(II) complexes have been reported to bind to bimolecular targets via other types of binding, including electrostatic interactions, and such investigations are being further developed.[4]

Most platinum complexes in clinical use as therapeutic agents contain amine (with at least one N−H bond) ligands.[5] However, analogous complexes containing phosphine ligands have also been investigated in therapeutic applications.[5b,6] The use of phosphine ligands in place of amines, as used in gold-containing complexes, have been successfully employed as therapeutic agents.[6,7] Considerable efforts have been made during the past three decades to synthesize novel complexes of platinum to overcome the shortcomings associated with cisplatin. Toward this goal, utilizing a rational design approach may provide the most effective means of discovering more clinically relevant platinum complexes.[2c] A promising example of these attempts is the discovery of cyclometalated platinum(II) complexes which have recently been investigated as anticancer drugs.[6,8] The biphosphine ligands bis(diphenylphosphino)methane, dppm = $Ph_2PCH_2PPh_2$, and to a lesser extent, its amine analogous bis(diphenylphosphino)amine, dppa = $Ph_2PNHPPh_2$, are versatile and robust ligands that are known to have different coordinating abilities.[9] Whether these coordinating capabilities play a role in augmenting the therapeutic activity of platinum complexes have yet to be understood.

The ubiquitin-proteasome pathway plays an essential role in critical cellular processes including cell cycle progression, differentiation, apoptosis, and signal transduction.[10] Its primary function is to degrade damaged, mutated, or misfolded proteins, which is vital in regulating cellular function.[11,12] Proteins marked for degradation are first tagged with a chain of ubiquitin molecules and translocated to the 26S proteasome.[13,14] The enzymatic activity of the 26S proteasome is mediated by the 20S proteasome that contains three pairs of catalytic sites responsible for its chymotrypsin-, trypsin-, and caspase-like activities.[15] Because inhibition of the proteasomal chymotrypsin-like activity is associated with tumor cell apoptosis, targeting the ubiquitin-proteasome pathway has become an

Received: December 18, 2010
Published: August 04, 2011

dx.doi.org/10.1021/jm2006832 | *J. Med. Chem.* 2011, 54, 6166–6176

Scheme 1

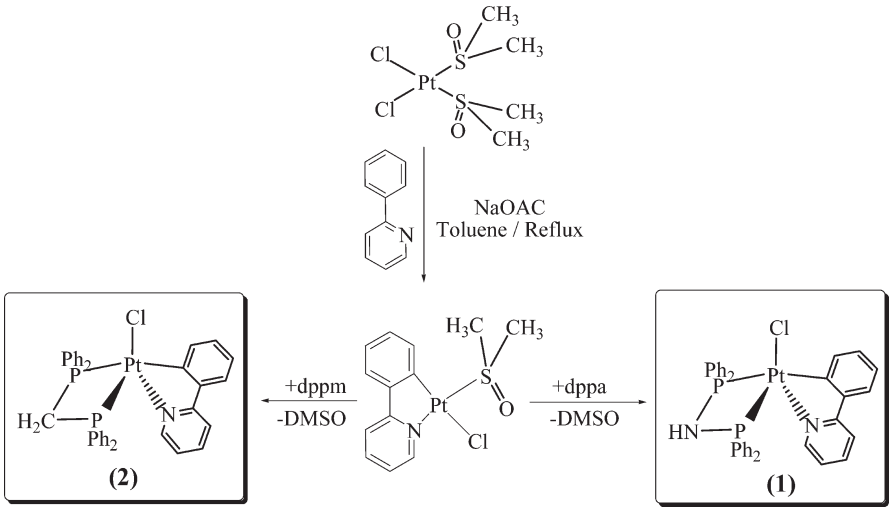

important target in cancer therapy.[16] Indeed, this concept was validated in 2003 when bortezomib became the first proteasome inhibitor approved by the Food and Drug Administration as an anticancer drug.[17,18] However, due to the appearance of toxicity and drug resistance coupled with limited activity toward solid tumors, efforts have been ongoing to develop novel proteasome inhibitors that address these shortcomings.

Many transition metal complexes are known to bind to DNA via both coordinative and noncovalent interactions. Noncovalent DNA interactions include intercalative, electrostatic, and groove (surface) binding outside of the DNA helix.[19] The study of noncovalent interactions of substitution inert transition metal complexes with DNA is an area of intense interest, owing to their photochemical properties and potential applications as new anticancer agents.[20] Additionally, the unique properties of metal complexes may also allow coordination of biological molecules other than DNA that may have significant clinical relevance.

In the present study, we investigated the biological activity of two five coordinated cyclometalated platinum(II) complexes containing either dppa or dppm ligands. Our results show that both platinum complexes exhibit potent anticancer activity under in vitro and in vivo conditions with activity superior to cisplatin. Interestingly both complexes showed proteasome inhibitory activity toward purified 20S proteasome and intact 26S proteasome in human breast cancer cells. Inhibition of proteasomal chymotrypsin-like activity by these platinum complexes was associated with apoptosis induction in these breast cancer cells. Importantly, preliminary studies show these platinum complexes could inhibit tumor growth in a mouse xenograft model with a more favorable toxicity profile compared to cisplatin. On the basis of the inherent luminescence activities of these complexes, we have suggested a binding mode to DNA and also a relationship between the structure of the complexes and their antitumor effects as it relates to their proteasome-inhibitory effects.

RESULTS AND DISCUSSION

Synthesis and Characterization of the Complexes. Two cyclometalated platinum(II) complexes [Pt(C^N)Cl(dppa)], **1**, and [Pt(C^N)Cl(dppm)], **2**, in which C^N = deprotonated 2-phenylpyridine, dppa = bis(diphenylphosphino)amine, or dppm = bis(diphenylphosphino)methane, were used to investigate their biological activities. As is depicted in Scheme 1, the complexes **1** or **2** were prepared from the reaction of the starting Pt^{II} complex [Pt(C^N)Cl(DMSO)], DMSO = dimethylsulfoxide, with 1 equiv of dppa or dppm, respectively. The complexes in solution were fully characterized by multi nuclear 1 and 2D NMR spectroscopy, and the details are described in the Experimental Section.

In the $^{31}P\{^1H\}$ NMR spectrum of complex [Pt(C^N)Cl(dppa)], **1**, two sharp doublets were observed, one at δ = 14.3 with ^1J(PtP) = 3426 Hz and ^2J(PP) = 40 Hz for the P atom *trans* to N and the other at δ = 32.7 with ^1J(PtP) = 1466 Hz and ^2J(PP) = 40 Hz for the P atom *trans* to C, confirming that dppa in complex **1** is chelated. In the ^1H NMR spectrum of complex **1** there are three notable signals appearing in low field region of the spectrum that are coupled to the platinum center. The two signals at δ = 8.58 and δ = 7.31 are attributed to the C−H group adjacent to N of the C^N ligand, i.e. H^6, and the C−H of phenyl group adjacent to the ligating carbon of C^N ligand, i.e. $H^{3'}$, respectively, confirming that apart from dppa, the C^N ligand is also chelated. The third signal, appearing at a significantly high chemical shift of δ = 11.63, is assigned to the NH group of dppa. The latter signal has a large ^1J(PtH) value of 125.3 Hz, supporting the formation of uncommon strong intermolecular N−H···Pt hydrogen bonding. Consistently, upon dilution, decreasing or increasing temperature or changing the solvent (even to those having high coordinating abilities such as DMSO-d_6 or CD_3CN), the signal for NH proton of dppa was clearly observed, with slight shifting and almost the same coupling constant.

In the $^{31}P\{^1H\}$ NMR spectrum of complex [Pt(C^N)Cl(dppm)], **2**, the P atom *trans* to C appeared as a doublet at δ = −25.6 ppm with ^1J(PtP) =1383 Hz that is coupled to the second dppm P atom (the one *trans* to N) with ^2J(PP) = 38 Hz. The P atom *trans* to N however appeared as a broad signal at δ = −33.6 ppm, with a much higher value of ^1J(PtP) = 3394 Hz, due to the *trans* influence of C being far greater than that of the N ligand, supporting that the dppm ligand being chelated in the complex **2**. In the ^1H NMR spectrum of complex [Pt(C^N)Cl(dppm)], **2**, the two signals at δ = 8.24 and δ = 6.92 are attributed to the C−H

dx.doi.org/10.1021/jm2006832 |*J. Med. Chem.* 2011, 54, 6166–6176

Scheme 2

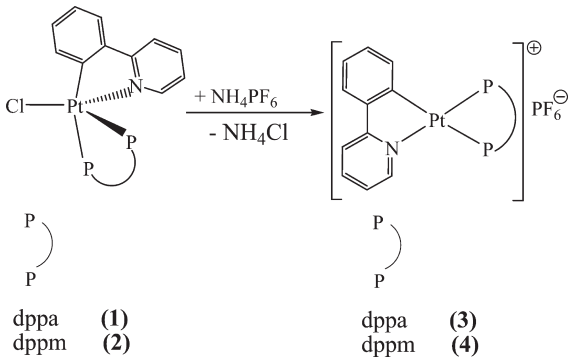

group adjacent to N of the C^N ligand, i.e. H^6, and the C−H of phenyl group adjacent to the ligating carbon of C^N ligand, i.e. $H^{3'}$, respectively; the data confirm that aside from dppm, the C^N ligand is also chelated. Unlike the N−H···Pt intermolecular interaction suggested to occur for complex **1**, any similar interaction of type C−H···Pt was not detected for the analogous complex **2**, probably due to less acidic nature of C−H group of dppm as compared to that of the N−H group of dppa. All these plus the conductivity measurements, describing that the complexes are not ionic even at low temperatures (see below), strongly support that the structure of the complexes **1** and **2** in solution should be pentacoordinated.

When the complexes **1** and **2** were reacted with NH_4PF_6, the chlorine ligands were removed from the coordination sites and the cationic complexes $[Pt(C^N)(dppa)]^+PF_6^-$, **3**, and $[Pt(C^N)(dppm)]^+PF_6^-$, **4**, respectively, were yielded (Scheme 2) in each of which the PF_6^- counteranion has no coordinating ability.

Typically, In the $^{31}P\{^1H\}$ NMR spectrum of complex $[Pt(C^N)(dppa)]^+PF_6^-$, **3**, two sharp doublets were observed, one at $\delta = 19.0$ with $^1J(PtP) = 3475$ Hz and $^2J(PP) = 47$ Hz for the P atom *trans* to N and the other at $\delta = 36.9$ with $^1J(PtP) = 1495$ Hz and $^2J(PP) = 47$ Hz for the P atom *trans* to C. The conductivity measurements, for the complexes **3** and **4** (see below), revealed that the complexes should be ionic in solution.

The molar conductances of 10^{-3} M solutions of complexes **1**−**4** in solution at different temperatures were measured. The values obtained for the complexes **3** and **4**, with PF_6^- counterions, in dichloromethane (+20 °C) were 140 and 130 Ω^{-1} cm^2 mol^{-1}, respectively, complying with the complexes being 1:1 electrolytes; the reported values for 10^{-3} M solution of 1:1 electrolyte compounds are between 100 to 140 Ω^{-1} cm^2 mol^{-1}.[21] In contrast, for the complexes **1** and **2** the values in dichloromethane (+20 °C) were 0.5 and 7.0 Ω^{-1} cm^2 mol^{-1}, respectively, confirming that the complexes are nonionic. The data support that the complexes **1** and **2** in solution ought to be neutral involving the coordination of Cl^- to form the related pentacoordinated complexes as shown in Scheme 1, rather than having cationic structures with square-planar geometry around the metallic centers, i.e. $[Pt(C^N)(dppa)]Cl$ and $[Pt(C^N)(dppm)]Cl$, respectively.

Effect of Complexes 1 and 2 on Cell Proliferation in Human Breast Cancer Cells. In the current study, we investigated the effect of these platinum complexes and, more importantly, the cellular target responsible for their underlying biological activity. We first tested the growth-inhibitory effect of the complexes **1** and **2** toward the highly aggressive breast cancer MDA-MB-231 cell line by performing an MTT assay, MTT = 3-(4,5-dimethyl-2-thiazolyl)-2,5-diphenyl-2*H*-tetrazolium bromide. We found that both compounds were similarly capable of inhibiting cell proliferation with IC_{50} values ~3.0 μmol/L (Figure 1). Furthermore, when cells were treated with 7.5 μmol/L of either of the platinum complexes, nearly 100% cell proliferation was inhibited (Figure 1). As a comparison, cisplatin was unable to inhibit cell proliferation at 100 μmol/L under the same experimental conditions (Figure 1).

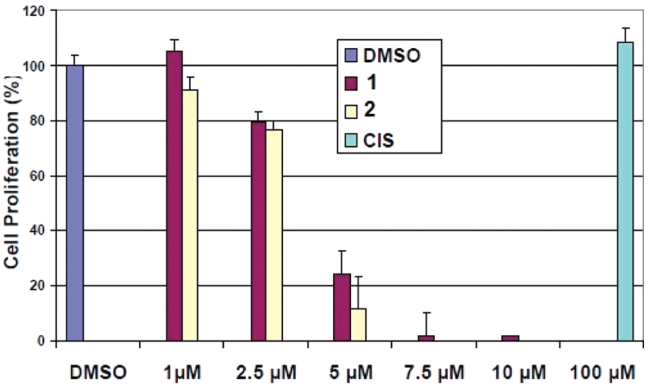

Figure 1. Antiproliferative effects of Pt-complexes **1** and **2** toward MDA-MB-231 breast cancer cells.

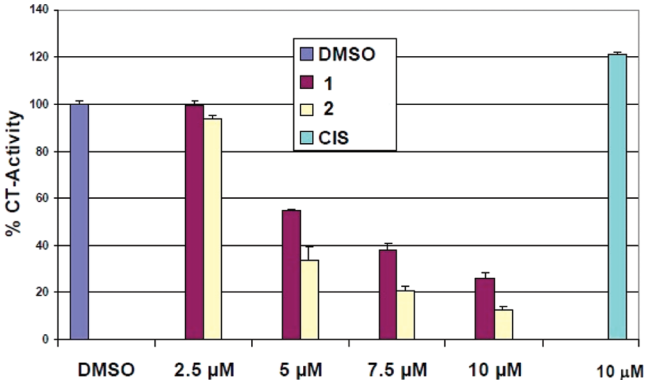

Figure 2. Inhibition of the proteasomal chymotrypsin-like activity of purified rabbit 20S proteasome by complexes **1** and **2**. Cisplatin was used as a negative control.

Inhibition of the Chymotrypsin-Like Activity of a Purified 20S Proteasome by Complexes 1 and 2. We have previously[22−24] shown that different metal-containing complexes can inhibit the proteasome activity and therefore hypothesized that the platinum complexes tested here with the correct choice of ligands and structure might be similarly capable of targeting and inhibiting the proteasome. To provide direct evidence for this, we incubated a purified rabbit 20S proteasome with the complexes **1** and **2**, and cisplatin followed by measurement of the proteasomal chymptrypsin-like(CT-like) activity. We found that the CT-like activity was significantly inhibited by both compounds **1** and **2** with similar potencies (IC_{50} = ~ 6.0 and 4.0 μmol/L, respectively) (Figure 2). In comparison, cisplatin at 10 μmol/L failed to inhibit the proteasomal chymotrypsin-like activity (Figure 2).

dx.doi.org/10.1021/jm2006832 |*J. Med. Chem.* 2011, 54, 6166–6176

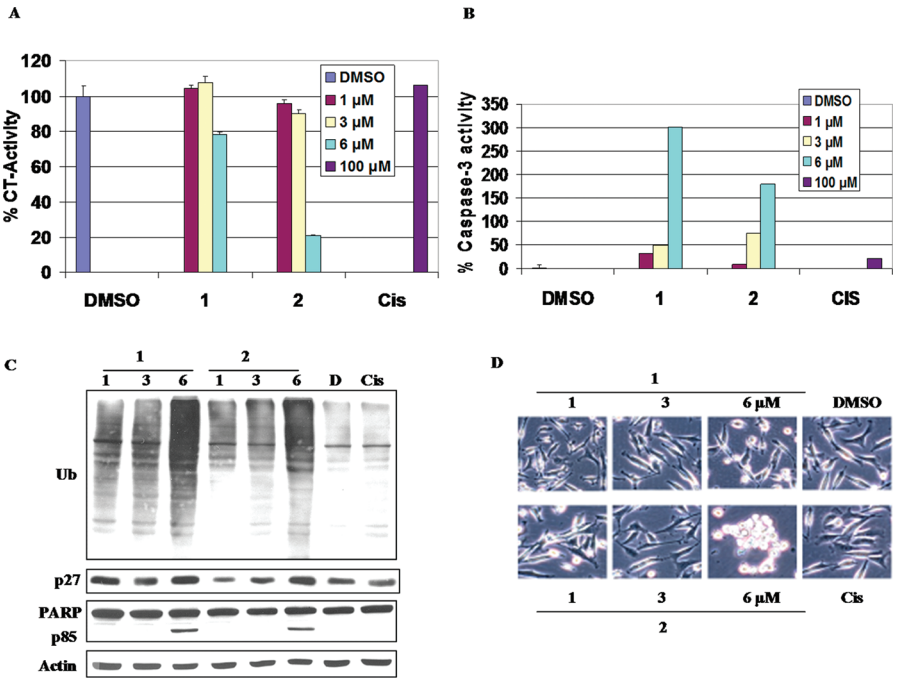

Figure 3. Inhibition of the proteasomal chymotrypsin-like activity by Pt complexes **1** and **2** is associated with apoptosis in intact MDA-MB-231 cells. (A) The cells were treated with complexes **1** or **2** at the indicated concentrations (1, 3, 6 μM) for 24 h, collected, and analyzed for the chymotrypsin-like activity. (B) Western blot analysis for accumulation of ubiquitinated proteins, proteasome target protein (p27), PARP cleavage in the cell extracts after 24 h treatment. (C) Activation of caspase 3 activity. (D) Induction of apoptosis by complexes **1** and **2** in MDA-MB-231 cells treated with indicated concentrations of either complex. Apoptotic morphological changes visualized by phase-contrasting imaging. Magnification ×100.

Pt Complexes 1 and 2 Inhibit the Chymotrypsin-Like Activity and Induce Apoptotic Cell Death in Human Breast Cancer Cells. To test whether these Pt containing complexes were active proteasome-inhibitory compounds in intact breast cancer cells, highly aggressive MDA-MB-231 breast cancer cells were treated with different concentrations of complexes **1** or **2** for 24 h. DMSO and cisplatin were used as controls under the same experimental conditions. Following treatment, cells were collected and protein extracts were used to measure levels of the proteasomal chymotrypsin-like activity, ubiquitinated proteins, and the proteasome target protein p27. We found that complex **2** only slightly inhibited the chymotrypsin-like activity at both 1 and 3 μM. However, the proteasomal activity was inhibited ~80% by complex **2** at 6 μM (Figure 3A). Consistently, the accumulation of ubiquitinated proteins and the proteasome target protein p27 was observed in cells treated with complex **2** (Figure 3B). Additionally, complex **1** was able to inhibit the proteasomal activity but to a much lesser extent (Figure 3A). Although proteasomal activity was only inhibited ~23% by 6 μM of compound **1**, this effect still resulted in higher levels of ubiquitinated proteins (Figure 3B). In parallel, treatment with cisplatin at 100 μM did not cause inhibition of proteasomal activity (Figure 3 A, B).

It has been shown that inhibition of the proteasomal chymotrypsin-like activity is associated with apoptosis induction in tumor cells.[25] To investigate whether proteasome inhibition results in apoptosis, morphological changes, caspase 3 activation, and apoptosis-associated PARP cleavage were assessed. Treatment with complexes **1** and **2** resulted in PARP cleavage, associated with the production of the p85 fragment at the highest concentration tested (Figure 3B). Because visible levels of PARP cleavage by platinum complexes are apparent, you would expect to see higher levels of caspase 3 activity. Consistent with this observation, PARP cleavage was accompanied by increasing levels of caspase 3 activity. Cells treated with complexes **1** and **2** resulted in a 300% and 180% increase in caspase 3 activity, respectively (Figure 3C). In comparison, only ~35% increase in caspase 3 activity was apparent in cells treated with cisplatin compared to DMSO control (Figure 3C). Furthermore apoptotic morphological changes (shrunken cells and characteristic apoptotic blebbing) were present in cells treated with complexes **1** and **2** at the highest concentration tested (Figure 3D). Taken together, these results show that complexes **1** (to a lesser extent) and **2** are able to inhibit the proteasomal chymotrypsin-like activity at varying levels of potency, resulting in apoptosis in human breast cancer MDA-MB-231 cells.

Pt Complexes 1 and 2 Inhibit the Growth of Breast Cancer Xenografts Associated with Proteasome Inhibition and Apoptosis Induction in Vivo. Our data described above clearly show that platinum complexes **1** and **2** can target and inhibit the tumor proteasome under cell-free conditions and in cultured breast cancer cells at varying potencies associated with decreased cell proliferation and increased cell death. To determine whether complexes **1** and **2** could induce apoptosis and inhibit tumor growth associated with proteasome inhibition in vivo, we conducted a preliminary study by first implanting MDA-MB-231 breast cancer cells sc in nude mice. When the tumors became palpable, the mice were injected sc daily with solvent or 2.5 mg/kg of either platinum complex **1**, **2**, or cisplatin for 29 days. At the end of the trial, the mice were sacrificed and their tumor tissue was used for immnostaining. Preliminary results showed that treatment of breast tumor xenografts by platinum complexes **1** and **2** was associated with significant reduction in tumor growth. Although cisplatin treatment also caused significant tumor

dx.doi.org/10.1021/jm2006832 |J. Med. Chem. 2011, 54, 6166–6176

growth inhibition, its toxicity was apparent as evidenced by loss of body weight compared to solvent control. In sharp contrast, platinum complexes **1**- and **2**-treated mice showed no visible signs of toxicity, as indicated by a relatively stable body weight compared to solvent control.

To determine if apoptosis associated with proteasomal inhibition was the predominant factor responsible for tumor growth inhibition, prepared tumor samples were used for p27, H&E, and TUNEL staining (Figure 4), H&E = hematoxylin and eosin, TUNEL = terminal deoxyribonucleotidyl transferase-mediated dUTP nick end-labeling. Induction of apoptosis was confirmed in tumors treated with platinum complexes **1** and **2** compared to control-treated tumors by measurable levels of condensed apoptotic nuclei detected in H&E staining and the presence of TUNEL-positive cells (Figure 4). Complex **2**-treated tumors contained low levels of apoptotic markers, whereas complex-**1** treated tumors contained much higher levels of apoptotic indices (Figure 4). Additionally, low levels of p27 were detected in tumors treated with complex **1**. It is important to note that although complex **2** exhibited higher potency under in vitro and cell culture conditions, complex **1** showed higher apoptotic indices under in vivo conditions. Taken together, our results show that suppression of cell proliferation, and apoptotic cell death induction by complexes **1** and **2** in vitro, is associated with tumor growth ablation and appearance of apoptotic indices in vivo.

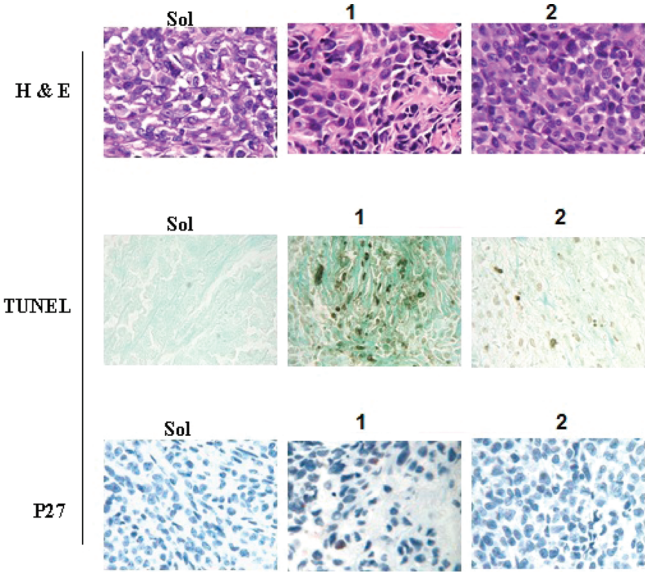

Figure 4. Hematoxylin and eosin (H&E) staining, TUNEL, and p27 assays using harvested mouse tumor samples treated with Pt-complexes **1** or **2**. Tumors were collected after a 29-day treatment, and the prepared tissue slides were used for immunostaining with H&E and TUNEL staining assays. Apoptotic-condensed nuclei and TUNEL-positive cells were found in tumor tissue from mice treated with platinum complex **1** or **2**. Magnification: ×400.

DNA-Binding Studies. *Native Fluorescence of Complexes.* The fluorescence spectra of a 50 μM solution of the complexes **1** and **2** in the absence and presence of a fixed amount of DNA are shown in Figure 5. The complexes exhibit twin emission bands in the range 460−570 nm (λ_{ex} = 312 nm). Upon additions of DNA, the fluorescence emission intensity of both platinum complexes grew steadily. The result suggests that the stronger enhancement of the fluorescence intensity may be largely due to the interaction between adjacent base pairs of DNA and the complexes. An increase in the molecule's planarity and a decrease of the collisional frequency solvent molecules with the complexes usually lead to emission enhancement. The results agree with those observed for other intercalators.[26]

EB−DNA Quenching Assay. In an effort to understand the interaction pattern of the complexes with DNA more clearly, fluorometric competitive binding experiment was carried out using ethidium bromide (EB) as a probe. The intrinsic fluorescence intensities of DNA and that of EB in Tris−HCl buffer are low. However, EB emits intense fluorescent light in the presence of DNA due to its strong intercalation between the adjacent DNA base pairs.[27] If the complexes can intercalate into DNA, the binding sites of DNA available for EB will be decreased, hence the fluorescence intensity of EB will be quenched. This is proof that the complexes intercalate between base pairs of DNA.[27,28] The quenching extent of fluorescence of EB−DNA is used to determine the extent of binding between the complex and DNA. The emissions spectrum of EB binding to DNA in the absence and presence of the complexes is given in Figure 6. The addition of the complexes to DNA pretreated with EB causes an appreciable reduction in the emission intensity, indicating the replacement of EB by the complexes.[29] As observed, complex **2** represented a slightly more pronounced quenching effect on fluorescence intensity of EB−DNA, underscoring its tighter binding to DNA as compared to complex **1**. We believe that in aqueous media the complexes **1** and **2** remain pentacoordinated upon attacking DNA and so they really act as drugs and not prodrugs, with the active drug being cationic complexes with square planar geometry around the metallic center, i.e. $[Pt(C^N)(dppa)]^+$ and $[Pt(C^N)(dppm)]^+$, respectively. Consistently, when the four-coordinated cationic complexes $[Pt(C^N)(dppa)]^+PF_6^-$, **3**, and $[Pt(C^N)(dppm)]^+PF_6^-$, **4**, were reacted with DNA, the fluorescence behaviors, as shown in Figure 6, were significantly different as compared with those of five coordinated complexes **1** and **2**. Thus, relative to fluorescence of EB−DNA initial adduct (taken as 100%), the fluorescence values of complexes **1** and **2** are significantly lower, being

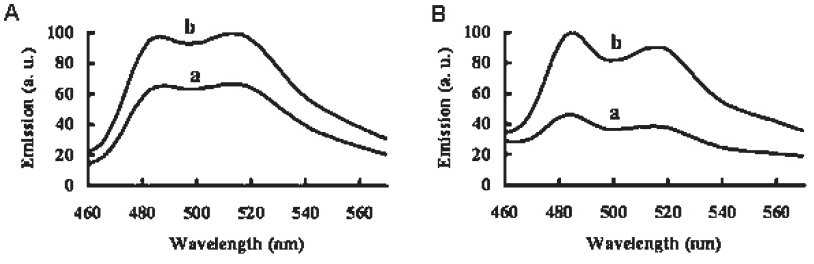

Figure 5. (A) Emission spectra of complexes (50.0 μM) in the absence (a) and presence (b) of DNA (100.0 μM): (A) complex **1**, (B) complex **2**.

dx.doi.org/10.1021/jm2006832 |J. Med. Chem. 2011, 54, 6166–6176

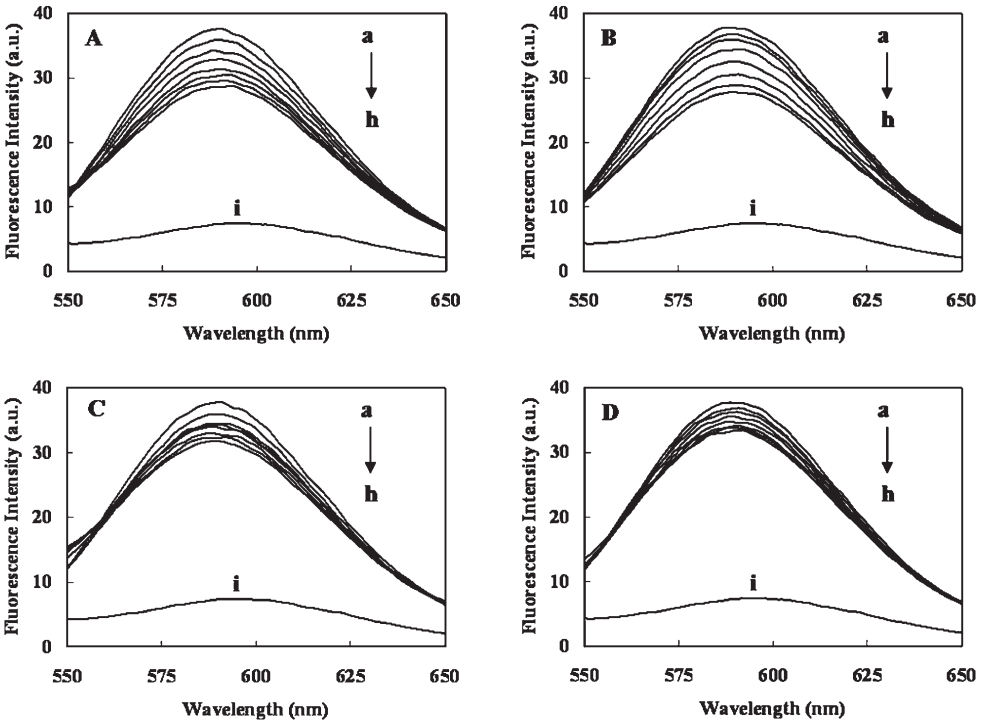

Figure 6. Emission spectrum of EB, shown by i, EB bound to DNA; a, and EB−DNA in the presence of different added amounts of platinum(II) complexes (b−h: 5.0, 9.9, 14.8, 19.6, 24.4, 29.1, and 33.8 μM, respectively). (A) complex **1**, (B) complex **2**, (C) complex **3**, (D) complex **4**. [EB] = 4.0 μM, [DNA] = 40.0 μM, λ_{ex} = 525 nm.

76.0% and 73.6%, respectively. The corresponding values for the complexes **3** and **4** were quite different (as compared with those for complexes **1** and **2**), being 84.2% and 89.0%, respectively.

CONCLUDING REMARKS

According to multinuclear 1D and 2D NMR spectroscopy and conductometric determinations, the complexes [Pt(C^N)-Cl(dppa)], **1**, and [Pt(C^N)Cl(dppm)], **2**, appear to be neutral with five-coordinated geometry around the platinum centers; note also that in the ^{195}Pt NMR spectra of complexes **1** and **2**, the related signals are located in the region expected for the five-coordinated Pt^{II} complexes.[35a,b] In contrast, the complexes $[Pt(C^N)(dppa)]^+PF_6^-$, **3**, and $[Pt(C^N)(dppm)]^+PF_6^-$, **4**, in which the PF_6^- counterion has no coordinating ability, are indicated to have square planar geometry around the metallic center.

The effects of complexes **1** and **2** were tested toward purified 20S and intact human breast cancer cells, under both cell culture conditions and mice-bearing xenografts. The results indicate that both complexes were able to significantly inhibit the proliferation of breast cancer cells at similar levels (IC_{50} = ∼ 3.0 μmol/L) (Figure 1). Additionally, associated with cell growth inhibition was a significant decrease in the chymotrypsin-like activity by complexes **1** and **2** (IC_{50} = ∼ 6 and 4 μmol/L, respectively) (Figure 2). When tested against the 26S proteasome of cultured breast cancer cells, complex **2** demonstrated higher proteasome inhibitory activity associated with cell death, as indicated by aberrant morphological changes (Figure 3A,B). Although both complexes were shown to indicate higher antitumor activities as compared to cisplatin under cell culture conditions, complex **1** was visibly less effective in terms of its proteasome-inhibitory capabilities. This may potentially be due to the formation of the intermolecular Pt···H−N hydrogen bonding that retards the platinum center to attack the N-terminal threonine of β-5. In addition, because complex **2** showed a higher binding affinity toward DNA as measured by fluorescence intensity (Figure 6), this finding may be valid toward other biological targets, including the proteasome, which showed a higher level of proteasome-inhibitory and apoptotic activity compared to complex **1** under cell culture conditions. However, under in vivo conditions, complex **1** showed higher levels of apoptotic indices, as indicated by H&E and TUNEL staining of mice tumor tissue. It is tempting to suggest the amine-containing biphosphine ligand of complex **1** may confer greater stability when complexed to the platinum center under in vivo conditions and may be less susceptible to metabolic inactivation. However, this is purely speculative and no firm conclusions could be established. All these data suggest using five-coordinate drug design strategy for the future development of platinum-containing complexes.[35]

It has been well detailed that Pt-containing complexes exert their biological effects primarily through the intercalation of DNA and ultimately triggering apoptotic cell death. However, in addition to their DNA binding properties, the current study proposes the cellular proteasome as a novel target for these biphosphine-containing platinum complexes that are at least partially responsible for their observed antitumor effects both in vitro and in vivo. Each of the complexes **1** or **2**, containing a robust biphosphine ligand, exhibits DNA binding capabilities and thus is a suitable platform for the design of novel platinum anticancer drugs. These complexes are quite stable in an S-donor media environment, such as DMSO, for considerable time, and the platinum centers are capable of accepting strong hydrogen bond. These unique properties of biphosphine platinum complexes **1** and **2** may hold potential in conferring a more favorable

dx.doi.org/10.1021/jm2006832 |*J. Med. Chem.* 2011, 54, 6166–6176

Scheme 3

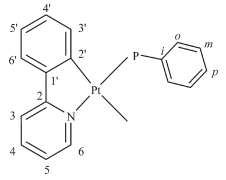

cellular distribution profile, which includes mitigating off-target effects, and resulting in lower toxicity levels as compared to conventional platinum drugs. However, this is purely speculative and further investigations are needed to validate their clinical potential. Nonetheless, the data observed suggest that platinum complexes containing biphosphine ligands as proteasome inhibitors hold significant potential to be further developed as potential anticancer drugs.

DNA binding studies confirm that in aqueous media the complexes **1** and **2** remain pentacoordinated upon attacking DNA, and so they really act as drugs and not prodrugs with the active drug being cationic complexes with square planar geometry around the metallic center.

EXPERIMENTAL SECTION

The ^{1}H, ^{31}P, and ^{195}Pt NMR and 2-D NMR spectra were recorded on a Bruker Avance DRX 500 MHz. References were TMS (^{1}H), H_3PO_4 (^{31}P), aqueous K_2PtCl_4 (^{195}Pt), and NH_4Cl(^{15}N). All the chemical shifts and coupling constants are in ppm and Hz, respectively. The conductivity measurements were performed using an ino-Lab Cond 720 conductometer. The reagents HC^N, dppm, and dppa were used as purchased from Aldrich, Merck, and Stream, respectively, without any further purification. [Pt(C^N)Cl(DMSO)] was prepared according to literature method.[30] Purities of the synthesized compounds are ≥98% as determined by elemental analysis in conjunction with using multinuclear NMR spectroscopy. All other chemicals and solvents were commercially available compounds. The labeling for NMR data is shown in Scheme 3.

3-[4,5-Dimethyltiazol-2-yl]-2,5-diphenyl-tetrazolium bromide (MTT), DMSO, and cisplatin were purchased from Sigma-Aldrich (St. Louis, MO). DMEM F/12, penicillin, and streptomycin were purchased from Invitrogen (Carlsbad, CA). Purified rabbit 20S proteasome was purchased from Boston Biochem (Cambridge, MA). Fluorogenic peptide substrates Suc-LLVY-AMC and Ac-DEVD-AMC (for the proteasomal chymotrypsin-like, and Caspase 3 activities, respectively) were from EMD Biosciences (San Diego, CA). Mouse monoclonal antibody against human poly(ADP-ribose) polymerase PARP was purchased from BD Biocsciences (San Diego, CA). Mouse monoclonal antibodies against p27, ubiquitin, goat polyclonal antibody against actin, and secondary antibodies were from Santa Cruz Biotechnology, Inc. (Santa Cruz, CA).

UV−Vis absorption spectra were measured on HP (model 8452A) photodiode array UV/vis using a 1.0 cm cell. Fluorescence spectra were recorded using Perkin−Elmer LS-55B fluorescence spectrophotometer (USA) with a 1.0 cm quartz cell. Both of the excitation and emission bandwidths were 10 nm and the scan rate was 1500 nm min^{-1}. The pH value was photometrically measured using a Metrohm 654 pH-meter equipped with a combined glass electrode (pH Electrode Blue Line 23 pH, Schott).

[Pt(C^N)Cl(dppa)], 1. To a solution of [Pt(C^N)Cl(DMSO)] (100 mg, 0.216 mmol) in acetone (5 mL) was added dppa (83.5 mg, 0.216 mmol). A light green−yellow precipitate was formed after a few min. This was stirred at RT for 1 h. The light green−yellow precipitate was filtered off, and the residue was washed with 1 mL of cold acetone and dried on oven at 60 °C. Yield 94.7% (161 mg). Anal. Calcd for $C_{35}H_{29}ClN_2P_2Pt\cdot H_2O$: C, 53.34; H, 3.96; N, 3.55. Found: C, 53.81; H, 3.88; N, 3.58%. Molar conductivity in CH_2Cl_2(10^{-3} M): at +20 °C = 0.5 Ω^{-1} cm^2 mol^{-1} and at +5 °C = 0.4 Ω^{-1} cm^2 mol^{-1}. ^{1}H NMR (500 MHz, CD_2Cl_2, 25 °C, 0.0325 molar, TMS): δ 7.06 [tt, ^{3}J(HH) = 7.4 Hz, ^{5}J(PH) = 1.6 Hz, 1H, $H^{4'}$ of C^N], 7.21 [t, ^{3}J(HH) = 7.2 Hz, 1H, $H^{5'}$ of C^N], 7.21 [t, ^{3}J(HH) = 7.6 Hz, 1H, H^{5} of C^N], 7.31 [td, ^{3}J(HH) = 7.6 Hz, ^{4}J(P_{trans}H) = 7.6 Hz, ^{4}J(P_{cis}H) = 4.1 Hz, ^{3}J(PtH) ≈ 54 Hz, 1H, $H^{3'}$ of C^N], 7.51 [dt, ^{3}J(HH) = 7.6 Hz, ^{4}J(PH) = 2.8 Hz, 4H, H^{m} of phenyl rings of PPh_2], 7.53 [dt, ^{3}J(HH) = 7.6 Hz, ^{4}J(PH) = 2.6 Hz, 4H, H^{m} of phenyl rings of PPh_2], 7.59 [dt, ^{3}J(HH) = 7.5 Hz, ^{5}J(PH) = 1.8 Hz, 2H, H^{p} of phenyl rings of PPh_2], 7.60 [dt, ^{3}J(HH) = 7.4 Hz, ^{5}J(PH) = 1.8 Hz, 2H, H^{p} of phenyl rings of PPh_2], 7.71 [d, ^{3}J(HH) = 7.8 Hz, 1H, $H^{6'}$ of C^N], 7.92 [ddd, ^{3}J(HH) = 7.1 Hz, ^{3}J(PH) = 12.7 Hz, ^{4}J(HH) = 1.4 Hz, 4H, H^{o} of phenyl rings of PPh_2], 7.95 [d, ^{3}J(HH) = 8.2 Hz, 1H, H^{3} of C^N], 8.01 [ddd, ^{3}J(HH) = 7.2 Hz, ^{3}J(PH) = 13.3 Hz, ^{4}J(HH) = 1.2 Hz, 4H, H^{o} of phenyl rings of PPh_2], 8.02 [t, ^{3}J(HH) = *not resolved*, overlapped with H^{o} of phenyl rings, 1H, H^{4} of C^N], 8.58 [broad dd, ^{3}J(PtH) ≈ 40 Hz, ^{4}J(PH) = 4.9 Hz, ^{3}J(HH) = 5.2 Hz, 1H, H^{6} of pyridine group], 11.63 [broad singlet, ^{1}J(PtH) = 125.3 Hz, NH fragment of dppa]; similar data were observed in the related ^{1}H NMR spectra at −14, +40, and +47 °C except shifting of NH group. ^{13}C NMR (125.77 MHz, CD_2Cl_2, 25 °C, TMS): δ 120.1 [s, ^{3}J(PtC) ≈ 34 Hz, C^{3} of C^N], 124.3 [d, ^{4}J(PC) = 5 Hz, $C^{6'}$ of C^N], 124.5 [d, ^{4}J(PC) = 3 Hz, C^{5} of C^N], 126.0 [s, $C^{5'}$ of C^N], 129.0 [d, ^{3}J(PC) = 13 Hz, C^{m} phenyl rings of PPh_2 fragments], 129.3 [d, ^{3}J(PC) = 11 Hz, C^{m} phenyl rings of PPh_2 fragments], 130.0 [dd, ^{1}J(PC) = 68 Hz, ^{3}J(PC) = 4 Hz, C^{ipso} phenyl rings of PPh_2 fragments], 131.2 [dd, ^{4}J(PC) = 9 Hz, ^{4}J(PC) = 4 Hz, $C^{4'}$ of C^N], 132.1 [d, ^{4}J(PC) = 2 Hz, C^{p} phenyl rings of PPh_2 fragments], 132.3 [dd, ^{1}J(PC) = 49 Hz, ^{3}J(PC) = 3 Hz, C^{ipso} phenyl rings of PPh_2 fragments], 132.4 [d, ^{4}J(PC) = 2 Hz, C^{p} phenyl rings of PPh_2 fragments], 132.6 [d, ^{2}J(PC) = 14 Hz, C^{o} phenyl rings of PPh_2 fragments], 133.2 [d, ^{2}J(PC) = 14 Hz, C^{o} phenyl rings of PPh_2 fragments], 139.0 [dd, ^{3}J(PC) = 6 Hz, ^{3}J(PC) = 5 Hz, $C^{3'}$ of C^N], 140.8 [s, C^{4} of C^N], 147.5 [s, $C^{1'}$ of C^N], 153.2 [d, ^{2}J(PtC) = 22 Hz, ^{3}J(PC) = 9 Hz, C^{6} of C^N], 157.5 [d, ^{2}J(PC) = 109 Hz, ^{1}J(PtC) = *not observed*, $C^{2'}$ of C^N], 167.0 [dd, ^{3}J(PC) = 3 Hz, ^{3}J(PC) = 5 Hz, C^{2} of C^N]. ^{31}P NMR (202 MHz, CD_2Cl_2, 25 °C, H_3PO_4): δ 14.3 (d, ^{1}J(PtP) = 3426 Hz, ^{2}J(PP) = 40 Hz P *trans* to N), 32.7 (d, ^{1}J(PtP) = 1466 Hz, ^{2}J(PP) = 40 Hz, P *trans* to C). ^{15}N NMR (50 MHz, CD_2Cl_2, 25 °C, NH_4Cl): δ 52.5 (resolved from N−H HSQC). ^{195}Pt-NMR (107 MHz, CD_2Cl_2, 25 °C, $K_2[PtCl_4]$): δ −2454 (dd, ^{1}J(PtP) = 3422 Hz, P *trans* to N, ^{1}J(PtP) = 1476 Hz, P *trans* to C). Selected solution (CH_2Cl_2) Far-IR peaks (KBr): 564, 516, 501, and 454 cm^{-1}. ESI-mass in methanol: m/z 734.1 $[M - Cl]^+$.

[Pt(C^N)Cl(dppm)], 2. To a solution of [Pt(C^N)Cl(DMSO)] (100 mg, 0.216 mmol) in acetone (5 mL) was added dppm (83.0 mg, 0.216 mmol). After a few min a light green−yellow precipitate was formed. The mixture was stirred at RT for 1 h. The light green−yellow precipitate was filtered off, and the residue was washed with 1 mL of cold acetone and dried on oven. Yield 93.5% (159 mg); melting point >260 °C. Anal. Calcd for $C_{36}H_{30}ClNP_2Pt.H_2O$: C, 54.93; H, 4.10; N, 1.78. Found: C, 54.87; H, 3.97; N, 1.81%. Molar conductivity (10^{-3} M): at +20 °C = 7.0 Ω^{-1} cm^2 mol^{-1}, at +4 °C = 6.1 Ω^{-1} cm^2 mol^{-1}. NMR in $CDCl_3$: δ (^{1}H) = 4.99 [t, ^{2}J(PH) = 4.8 Hz, ^{3}J(PtH) = 20.0 Hz, 2H, CH_2 fragment of dppm ligand], 6.84 (t, ^{3}J(HH) = 7.3 Hz, 1H, $H^{4'}$ of C^N), 6.92 (td, ^{3}J(HH) = 7.5 Hz, ^{4}J(P *trans* H) = 7.5 Hz, ^{4}J(P *cis* H) = 3.5 Hz, ^{3}J(PtH) ≈ 40 Hz, 1H, $H^{3'}$ of C^N), 7.07 (t, ^{3}J(HH) = 7.6 Hz, 1H, $H^{5'}$ of C^N), 7.18 (t, ^{3}J(HH) = 6.4 Hz, 1H, H^{5} of C^N), 7.40 (t, ^{3}J(HH) = 7.7 Hz, 8H, H^{m} of phenyl rings of PPh_2), 7.42 (t, ^{3}J(HH) = 8.6 Hz, 2H, H^{p} of phenyl rings of PPh_2), 7.64 (d, ^{3}J(HH) = 7.9 Hz, 1H, $H^{6'}$ of C^N), 7.68 (dd, ^{3}J(HH) = 7.3 Hz, ^{3}J(PH) = 12.3 Hz, 4H, H^{o} of phenyl rings of PPh_2), 7.83 (dd, ^{3}J(HH) = 7.3 Hz, ^{3}J(PH) = 13.3 Hz, 4H,

H^o of phenyl rings), 7.94 (d, ^3J(HH) = 8.1 Hz, 1H, H^3 of C^N), 8.10 (t, ^3J(HH) = 7.8 Hz, 1H, H^4 of C^N), 8.24 (broad, ^3J(PtH) ≈ 30 Hz, 1H, H^6 of pyridine group). ^{13}C NMR (125.77 MHz, $CDCl_3$, 25 °C, TMS): δ 46.3 [t, ^1J(PC) = 36 Hz, CH_2 of dppm], 120.6 [s, C^3 of C^N], 124.6 [d, ^4J(PC) = 5 Hz, $C^{6'}$ of C^N], 125.0 [bs, C^5 of C^N], 126.6 [s, $C^{5'}$ of C^N], 129.5 [d, ^3J(PC) = 12 Hz, C^m phenyl rings of PPh_2 fragments], 129.9 [d, ^3J(PC) = 11 Hz, C^m phenyl rings of PPh_2 fragments], 131.2 [dd, ^4J(PC) = 9 Hz, ^4J(PC) = 4 Hz, $C^{4'}$ of C^N], 132.4 [s, C^p phenyl rings of PPh_2 fragments], 132.7 [s, C^p phenyl rings of PPh_2 fragments], 133.3 [d, ^2J(PC) = 13 Hz, C^o phenyl rings of PPh_2 fragments], 133.9 [d, ^2J(PC) = 13 Hz, C^o phenyl rings of PPh_2 fragments], 138.3 [s, ^2J(PtC) = 8 Hz, $C^{3'}$ of C^N], 141.9 [s, C^4 of C^N], 147.6 [s, $C^{1'}$ of C^N], 152.2 [s, C^6 of C^N], 156.1 [d, ^2J(PC) = 105 Hz, ^1J(PtC) = *not observed*, $C^{2'}$ of C^N], 167.0 [s, C^2 of C^N]; δ(^{31}P) at +27 °C = −33.6 [broad, ^1J(PtP) = 3394 Hz, ^2J(PP) = *not resolved*, P *trans* to N], −25.6 [d, ^1J(PtP) = 1383 Hz, ^2J(PP) = 38 Hz, P *trans* to C]; δ(^{31}P) at +10 °C = −33.9 [d, ^1J(PtP) = 3376 Hz, ^2J(PP) = 40 Hz, P *trans* to N], −26.1 [d, ^1J(PtP) = 1401 Hz, ^2J(PP) = 39 Hz, P *trans* to C]; δ(^{31}P) at +60 °C = −25.2 [d, ^1J(PtP) = 1275 Hz, ^2J(PP) = 28 Hz, P *trans* to C]. ^{31}P NMR data in CD_2Cl_2: δ(^{31}P) at +25 °C = −33.9 [broad, ^1J(PtP) = 3416 Hz, ^2J(PP) = *not resolved*, P *trans* to N], −25.8 [d, ^1J(PtP) =1335 Hz, ^2J(PP) = 35 Hz, P *trans* to C]; δ(^{31}P) at −5 °C = −34.5 [d, ^1J(PtP) = 3372 Hz, ^2J(PP) = 40 Hz, P *trans* to N], −26.6 [d, ^1J(PtP) = 1411 Hz, ^2J(PP) = 38 Hz, P *trans* to C]; δ(^{31}P) at −30 °C = −34.9 [d, ^1J(PtP) = 3314 Hz, ^2J(PP) = 40 Hz, P *trans* to N], −27.2 [d, ^1J(PtP) = 1412 Hz, ^2J(PP) = 40 Hz, P *trans* to C]. δ(^{195}Pt) = −2389[dd, ^1J(PtP) = 3380 Hz, ^1J(PtP) = 1420 Hz]. Selected solution (CH_2Cl_2) far-IR peaks (KBr): 547, 504, and 453 cm^{-1}. ESI-mass in methanol: *m*/*z* 733.2 $[M - Cl]^+$.

[Pt(C^N)(dppa)]PF_6, 3. To a solution of [Pt(C^N)Cl(dppa)], **1**, (20 mg, 0.025 mmol), in dichloromethane (5 mL) was added NH_4PF_6 (6 mg, 0.037 mmol) and a few drops of distilled water (to help dissolving NH_4PF_6). A pale-yellow precipitate was formed after a few min. This was stirred at RT for 3 h. The solvent was removed by rotary evaporator to yield a pale-yellow residue, which was then dissolved in 3 mL of dichloromethane and filtered. Solvent was removed from the light-yellow filtrate by rotary evaporator and residue washed with diethyl ether and dried on oven at 80 °C. Yield 91.6% (20.5 mg). Anal. Calcd for $C_{35}H_{29}F_6N_2P_3Pt$: C, 47.79; H, 3.32; N, 3.18. Found: C, 47.70; H, 3.28; N, 3.22%. Molar conductivity (10^{-3} M) in dichloromethane (+20 °C): 140 Ω^{-1} cm^2 mol^{-1}. ^{1}H NMR (250 MHz, $CDCl_3$, 25 °C): δ 7.17−8.0 (the aromatic region of 2-phenylpyridine ligand, NH group and phenyl groups of dppa), 8.48 (broad s, 1H, H^6 of C^N group). ^{31}P NMR (202 MHz, $CDCl_3$, 25 °C, H_3PO_4): δ −144.2 [h, ^1J(PF) = 713 Hz, PF_6^- counterion], 19.0 [d, ^1J(PtP) = 3475 Hz, ^2J(PP) = 47 Hz, P *trans* to N], 36.9 [d, ^1J(PtP) = 1495 Hz, ^2J(PP) = 37 Hz, P *trans* to C].

[Pt(C^N)(dppm)]PF_6, 4. To a solution of [Pt(C^N)Cl(dppm)], **2**, (20 mg, 0.025 mmol) in dichloromethane (5 mL) was added NH_4PF_6 (6 mg, 0.037 mmol) and a few drops of distilled water (to help dissolving NH_4PF_6). A pale-yellow precipitate was formed after a few min. This was stirred at RT for 3 h. The solvent was removed by rotary evaporator to yield a pale-yellow residue, which was then dissolved in 3 mL of dichloromethane and filtered. The solvent of light-yellow filtrate was removed by rotary evaporator and residue washed with diethyl ether and dried on oven at 80 °C. Yield 96.0% (21.5 mg); melting point >260 °C. Anal. Calcd for $C_{36}H_{30}F_6NP_3Pt$: C, 49.21; H, 3.44; N, 1.59. Found: C, 49.45; H, 3.46; N, 1.62%. Molar conductivity (10^{-3} M) in dichloromethane (+20 °C): 130 Ω^{-1} cm^2 mol^{-1}. NMR in $CDCl_3$: δ(^{1}H) = 4.64 [m, ^3J(PtH) = 25.2 Hz, 2H, CH_2 fragment of dppm ligand], 6.95−8.04 [the aromatic region of 2-phenylpyridine ligand and phenyl groups of dppm], 8.38[broad s, 1H, H^6 of C^N group]. δ(^{31}P) = −144.2 [h, ^1J(PF) = 713 Hz, PF_6^- counterion], −34.2 [d, ^1J(PtP) = 3394 Hz, ^2J(PP) = 39 Hz, P *trans* to N], −26.5 [d, ^1J(PtP) = 1403 Hz, ^2J(PP) = 39 Hz, P *trans* to C].

Cell Culture and Cell Extract Preparation. MDA-MB-231 cells were grown in DMEM F/12 supplemented with 10% fetal bovine serum, 100 units/mL of penicillin, and 100 μg/mL of streptomycin. All cells were grown at 37 °C in a humidified incubator with atmosphere of 5% CO_2. A whole-cell extract was prepared as previously described.[31] Briefly, cells were harvested, washed with PBS twice, and homogenized in a lysis buffer (50 mM Tris-HCl (pH 8.0), 150 mM NaCl, 0.5% NP40 (v/v), and 0.5 mM phenylmethylsulfonyl fluoride) for 30 min at 4 °C. The lysates were then centrifuged at 12000 rpm for 12 min, and the supernatants were collected as whole cell extracts.

Analysis of the Proteasomal Activity in Purified 20S Proteasome. Purified rabbit 20S proteasome was incubated with 20 μmol/L of Suc-LLVY-AMC (EMD Chemicals, Gibbstown, NJ, USA), a fluorogenic substrate specific for chymotrypsin-like activity, in 100 μL of assay buffer [20 mmol/L Tris-HCl (pH 7.5)] in the presence of platinum complexes, cisplatin, or equivalent volume of solvent DMSO as control. After 2 h of incubation at 37 °C, inhibition of the proteasomal chymotrypsin-like activity was measured by production of hydrolyzed AMC groups. A Victor 3 multilabel counter (PerkinElmer, Boston, MA, USA) with an excitation filter of 380 nm and emission filter of 460 nm was used to measure fluorescence. Values plotted are calculated as change in fluorescence against solvent-treated controls and are the mean from triplicate experiments.

Proteasome and Caspase 3 Activity Assays in Intact Breast Cancer MDA-MB-121 Cells. MDA-MB-231 breast cancer cells were grown to 70−80% confluency, treated for 24 h, harvested, and used for whole cell extract preparation. Then 10 μg of extract was used for proteasomal activity, as described above, and 24 μg for caspase 3 activity. For the caspase 3 assay, the fluorgenic substrate Ac-DEVD-AMC (EMD Chemicals, Gibbstown, NJ, USA) was used, and fluorescence was measured using a Victor 3 multilabel counter (PerkinElmer, Boston, MA, USA) with an excitation filter of 380 nm and emission filter of 460 nm. Values plotted are means of triplicate experiments.

Cell Proliferation Assay. The MTT (3-(4,5-dimethylthiazol-2-yl)-2,5-diphenyltetrazolium bromide; Sigma-Aldrich, St. Louis, MO, USA) assay was used to determine the effects of platinum and other compounds on breast cancer cell proliferation. Cells were plated in a 96-well plate and grown to 70−80% confluency, followed by addition of each complex at the indicated concentrations. Stock solutions were made in the millimolar range in DMSO and were then diluted 1:1000 in RPMI-1640 medium supplemented with FBS and penicillin/streptomycin as previously described. After 24 h of incubation at 37 °C, inhibition of cell proliferation was measured as previously described.[31] Briefly, drug-containing media was removed and MTT in PBS (1 mg/mL) was added to wells and incubated at 37 °C for 4 h to allow for complete cleavage of the tetrazolium salt by metabolically active cells. MTT was then removed and 100 μL per well DMSO was added, followed by colorimetric analysis using a Victor 3 multilabel plate reader (PerkinElmer, Boston, MA, USA) at a wavelength of 560 nm. Absorbance values plotted are the mean from triplicate experiments.

Cellular Morphology Analysis. A Zeiss (Thornwood, NY) Axiovert 25 microscope was used for all microscopic imaging with phase contrast for cellular morphology.

Western Blot Analysis. MDA-MB-231 cells were treated, harvested, and lysed. Cell lysates (40 μg), prepared as previously described, were separated by SDS-PAGE and transferred to a nitrocellulose membrane, followed by visualization using the HyGLO chemiluminescent reagents (Denville, Metuchin, NJ). Western blot analysis was performed using specific primary antibodies against p27, ubiquitin, and actin (loading control) (Santa Cruz Biotechnology, Santa Cruz, CA, USA) as well as PARP (Biomol, Plymouth Meeting, PA, USA). Membranes were incubated in mouse secondary antibody for p27, ubiquitin, PARP, and goat secondary antibody for actin (Santa Cruz Biotechnology, Santa Cruz, CA, USA).

Terminal Deoxyribonucleotidyl Transferase-Mediated dUTP Nick End-Labeling (TUNEL) Assay. Tumor tissues were paraffin embedded and stained according to the manufacturer's instructions. Briefly, after deparaffinization and hydration, the tissue was incubated with working strength stop/wash buffer, conjugated with antidigoxigenenin, and then stained with peroxidase substrate. Finally, the tissue was mounted under a glass coverslip in permount and viewed under a microscope.

H&E Staining Assay. Paraffin-embedded sample slides were deparaffinized and hydrated and then stained with eosin for 1 min, followed by further rinsing, and coverslips were mounted onto slides with permount.

DNA-Intercalation Study. Herring sperm DNA was procured from TCI chemicals (Japan) and used without further purification. Its stock solution was prepared by dissolving solid DNA into doubly distilled water overnight, and its concentration was determined by absorption spectrometry, using the molar absorptivity ε_{260} = 6600 L mol^{-1} cm^{-1}.[32] Stock solution of DNA was stored at 4°C in the dark for no more than a week. The solution gave a ratio of >1.8 at A_{260}/A_{280}, indicating that DNA is sufficiently protein-free.[33] Ethidium bromide (EB) was prepared by dissolving its crystals (Sigma-Aldrich Biotech. Co.) in doubly distilled water and diluted to the required volume, and its concentration was determined assuming a molar extinction coefficient of 5450 L mol^{-1} cm^{-1} at 480 nm.[34] The stock solutions (3.0 mM) of the platinum complexes were prepared by dissolving the powder materials into appropriate amounts of DMSO solutions. All the measurements involving the interactions of the two metal complexes with DNA were carried out in buffer solution containing 50 mM Tris and 100 mM NaCl and adjusted to pH 7.4 with hydrochloric acid. All spectroscopic measurements were studied at RT and 5 min after addition of complexes.

AUTHOR INFORMATION

Corresponding Author

*For Q.P.D.: phone, (+1) 313-576-8301; E-mail, doup@karmanos.org. For M.R.: phone. (+98)711- 6137345; E-mail, rashidi@chem.susc.ac.ir. For B.H. phone, (+98)711- 6137360; E-mail: hemmatb@sums.ac.ir.

ACKNOWLEDGMENT

We thank Karmanos Cancer Institute 2009 Pilot project funding (to Q.P.D.), the National Cancer Institute (1R01CA-120009, 3R01CA120009-04S1, 1R21CA139386-01, to Q.P.D.), training grant from the National Cancer Institute (T32-CA009531 to M.F.), and the Shiraz University research council for financial support. H.S. thanks the Inorganic Institute of Vienna University for technical and financial support. Prof. Gerard van Koten is gratefully acknowledged for his helpful suggestions. We also appreciate S. Abedanzadeh for her help in performing some initial tests. We appreciate the reviewers' helpful suggestions.

ABBREVIATIONS USED

C^N, deprotonated 2-phenylpyridine; CT, chymotrypsin; dppa, bis(diphenylphosphino)amine; dppm, bis(diphenylphosphino)-methane; DMSO, dimethylsulfoxide; HC^N, 2-phenylpyridine; EB, ethidium bromide; ESI-Mass, electrospray ionization mass spectrometry; H&E, hematoxylin and eosin; IC_{50}, 50% inhibitory concentrations; MTT, 3-(4,5-dimethyl-2-thiazolyl)-2,5-diphenyl-2*H*-tetrazolium bromide; PARP, poly(ADP-ribose) polymerase; TUNEL, terminal deoxyribonucleotidyl transferase-mediated dUTP nick end-labeling

REFERENCES

(1) Rosenberg, B.; VanCamp, L.; Trosko, J. E.; Mansour, V. H. Platinum compounds: a new class of potent antitumour agents. *Nature* **1969**, *222*, 385–386.

(2) (a) Lovejoy, K. S.; Lippard, S. J. Nontraditional platinum compounds for improved accumulation, oral bioavailability, and tumor targeting. *Dalton Trans.* **2009**, 10651–10659. (b) Galanski, M.; Jakupec, M. A.; Keppler, B. K. Update of the Preclinical Situation of Anticancer Platinum Complexes: Novel Design Strategies and Innovative Analytical Approaches. *Curr. Med. Chem.* **2005**, *12*, 2075–2094. (c) Montana, A. M.; Batalla, C. The Rational Design of Anticancer Platinum Complexes: The Importance of the Structure−Activity Relationship. *Curr. Med. Chem.* **2009**, *16*, 2235–2260. (d) Hambley, T. W. Developing new metal-based therapeutics: challenges and opportunities. *Dalton Trans* **2007**, 4929–4937. (e) Kostova, I. Platinum complexes as anticancer agents. *Recent Pat. Anti-Cancer Drug Discovery* **2006**, *1*, 1–22. (f) Pasini, A.; Zunino, F. New Cisplatin Analogues—On the Way to Better Antitumor Agents. *Angew. Chem.* **1987**, *99*, 632–642. *Angew. Chem., Int. Ed. Engl.* **1987**, *26*, 615–624.

(3) (a) Cohen, S. M.; Lippard, S. J. Cisplatin: from DNA damage to cancer chemotherapy. *Prog. Nucleic Acid Res. Mol. Biol.* **2001**, *67*, 93–130. (b) Gibson, D. The mechanism of action of platinum anticancer agents—what do we really know about it? *Dalton Trans* **2009**, 10681–10689. (c) Arnesano, F.; Natile, G. Mechanistic insight into the cellular uptake and processing of cisplatin 30 years after its approval by FDA. *Coord. Chem. Rev.* **2009**, *253*, 2070–2081. (d) Zhu, G.; Lippard, S. J. Photoaffinity Labeling Reveals Nuclear Proteins That Uniquely Recognize Cisplatin-DNA Interstrand Cross-Links. *Biochemistry* **2009**, *48*, 4916–4925. (e) Jung, Y.; Lippard, S. J. Direct Cellular Responses to Platinum-Induced DNA Damage. *Chem. Rev.* **2007**, *107*, 1387–1407. (f) Lu, Q. B.; Kalantari, S.; Wang, C. R. Electron Transfer Reaction Mechanism of Cisplatin with DNA at the Molecular Level. *Mol. Pharmaceutics* **2007**, *4*, 624–628. (g) Mantri, Y.; Lippard, S. J.; Baik, H. Bifunctional Binding of Cisplatin to DNA: Why Does Cisplatin Form 1,2-Intrastrand Crosslinks with AG, But Not with GA? *J. Am. Chem. Soc.* **2007**, *129*, 5023–5030. (h) Kopyra, J.; Koenig-Lehmann, C.; Bald, I.; Illenberger, E. A Single Slow Electron Triggers the Loss of Both Chlorine Atoms from the Anticancer Drug Cisplatin: Implications for Chemoradiation Therapy. *Angew. Chem.* **2009**, *121*, 8044–8047. *Angew. Chem., Int. Ed.* **2009**, *48*, 7904–7907. (i) Reissner, T.; Schneider, S.; Schorr, S.; Carell, T. Crystal Structure of a Cisplatin-(1,3-GTG) Cross-Link within DNA Polymerase *η*. *Angew. Chem.* **2010**, *122*, 3142–3145.Reissner, T.Schneider, S.Schorr, S.Carell, T.Crystal Structure of a Cisplatin-(1,3-GTG) Cross-Link within DNA Polymerase *η*.*Angew. Chem., Int. Ed.* **2010**, *49*, 3077−3080.

(4) (a) Sanchez-Cano, C.; Hannon, M. J. Novel and emerging approaches for the delivery of metallo-drugs. *Dalton Trans* **2009**, 10702–10711. (b) Ndinguri, M. W.; Solipuram, R.; Gambrell, R. P.; Aggarwal, S.; Hammer, R. P. Peptide Targeting of Platinum Anti-Cancer Drugs. *Bioconjugate Chem.* **2009**, *20*, 1869–1878.

(5) (a) Miguel, P. J.; Roitzsch, M.; Yin, L.; Lax, P. M.; Holland, L.; Krizanovic, O.; Lutterbeck, M.; Schur-mann, M.; Fusch, E. C.; Lippert, B. On the many roles of NH_3 ligands in mono- and multinuclear complexes of platinum. *Dalton Trans* **2009**, 10774–10786. (b) Shi, J. C.; Yueng, C. H.; Wu, D. X.; Liu, Q. T.; Kang, B. S. Chiral Phosphine Ligands Derived from Sugars. 16. Design and Synthesis of Platinum Anticancer Compounds with Carbohydrate Ligand. *Organometallics* **1999**, *18*, 3796–3801. (c) Beret, E. C.; Pappalardo, R. R.; Marx, D.; Marcos, E. S. Characterizing Pt-Derived Anticancer Drugs from First Principles: The Case of Oxaliplatin in Aqueous Solution. *ChemPhysChem* **2009**, *10* (7), 1044–1052. (d) Monti, E.; Gariboldi, M.; Maiocchi, A.; Marengo, E.; Cassino, C.; Gabano, E.; Osella, D. Cytotoxicity of *cis*-Platinum(II) Conjugate Models. The Effect of Chelating Arms and Leaving Groups on Cytotoxicity: A Quantitative Structure−Activity Relationship Approach. *J. Med. Chem.* **2005**, *48*, 857–866. (e) Er, H. M.; Hambley, T. W. Enantioselectivity and stereoselectivity in the reactions of the enantiomers of the platinum complex [$PtCl_2$(ahaz)] (ahaz = 3(*R*)- or

3(*S*)-aminohexahydroazepine) with DNA. *J. Inorg. Biochem.* **2009**, *103*, 168–173. (f) Mackay, F. S.; Moggach, S. A.; Collins, A.; Parsons, S.; Sadler, P. J. Photoactive trans ammine/amine diazido platinum(IV) complexes. *Inorg. Chim. Acta* **2009**, *362*, 811–819. (g) Zhang, J.; Liu, L.; Gong, Y.; Zheng, X.; Yang, M.; Cui, J.; Shen, S. Synthesis, characterization and antitumor activity of new type binuclear platinum(II) complexes. *Eur. J. Med. Chem.* **2009**, *44*, 2322–2327. (h) Kasherman, Y.; Sturup, S.; Gibson, D. Trans labilization of am(m)ine ligands from platinum(II) complexes by cancer cell extracts. *J. Biol. Inorg. Chem.* **2009**, *14*, 387–399. (i) Wheate, N. J.; Collins, J. G. Multinuclear platinum complexes as anti-cancer drugs. *Coord. Chem. Rev.* **2003**, *241*, 133–145. (j) Najajreh, Y.; Prilutski, D.; Ardeli-Tzaraf, Y.; Perez, J. M.; Khazanov, E.; Barenholz, Y.; Kasparkova, J.; Brabec, V.; Gibson, D. Structure and Unique Interactions with DNA of a Cationic Trans-Platinum Complex with the Nonplanar Bicyclic Piperidinopiperidine Ligand. *Angew. Chem.* **2005**, *117*, 2945–2947. *Angew. Chem., Int. Ed.* **2005**, *44*, 2885–2887. (k) Chen, Y.; Heeg, M. J.; Braunschweiger, P. G.; Xie, W.; Wang, P. G. A Carbohydrate-Linked Cisplatin Analogue Having Antitumor Activity. *Angew. Chem., Int. Ed.* **1999**, *111*, 1882–1884. *Angew. Chem., Int. Ed.* **1999**, *38*, 1768–1769. (l) Boer, J.; Blount, K. F.; Luedtke, N. W.; Elson-Schwab, L.; Tor, Y. RNA-Selective Modification by a Platinum(II) Complex Conjugated to Amino- and Guanidinoglycosides. *Angew. Chem.* **2005**, *117*, 949–954. *Angew. Chem., Int. Ed.* **2005**, *44*, 927–932.

(6) Sun, R. W.Y.; Ma, D. L.; Wong, E. L. M.; Che, C. M. Some uses of transition metal complexes as anti-cancer and anti-HIV agents. *Dalton Trans.* **2007**, 4884–4892.

(7) (a) Eiter, L. C.; Hall, N. W.; Day, C. S.; Saluta, G.; Kucera, G. L.; Bierbach, U. Gold(I) Analogues of a Platinum−Acridine Antitumor Agent Are Only Moderately Cytotoxic but Show Potent Activity against Mycobacterium tuberculosis. *J. Med. Chem.* **2009**, *52*, 6519–6522. (b) Bagowski, C. P.; You, Y.; Scheffler, H.; Vlecken, D. H.; Schmitz, D. J.; Ott, I. Naphthalimide gold(I) phosphine complexes as anticancer metallodrugs. *Dalton Trans.* **2009**, 10799–10805. (c) Schuh, E.; Valiahdi, S. M.; Jakupec, M. A.; Keppler, B. K.; Chiba, P.; Mohr, F. Synthesis and biological studies of some gold(I) complexes containing functionalised alkynes. *Dalton Trans.* **2009**, 10841–10845.

(8) (a) Okada, T.; El-Mehasseb, I. M.; Kodaka, M.; Tomohiro, T.; Okamoto, K.; Okuno, H. Mononuclear Platinum(II) Complex with 2-Phenylpyridine Ligands Showing High Cytotoxicity against Mouse Sarcoma 180 Cells Acquiring High Cisplatin Resistance. *J. Med. Chem.* **2001**, *44*, 4661–4667. (b) El-Mehasseb, I. M.; Kodaka, M.; Okada, T.; Tomohiro, T.; Okamoto, K.; Okuno, H. Platinum (II) complex with cyclometalating 2-phenylpyridine ligand showing high cytotoxicity against cisplatin-resistant cell. *J. Inorg. Biochem.* **2001**, *84*, 157–158. (c) Edwards, G. L.; Black, D. St. C.; Deacon, G. B.; Wakelin, L. P. G. Effect of charge and surface area on the cytotoxicity of cationic metallointercalation reagents. *Can. J. Chem.* **2005**, *83*, 969–979. (d) Edwards, G. L.; Black, D. St. C.; Deacon, G. B.; Wakelin, L. P. G. In vitro and in vivo studies of neutral cyclometallated complexes against murine leukæmias. *Can. J. Chem.* **2005**, *83*, 980–989. (e) Ruiz, J.; Lorenzo, J.; Sanglas, L.; Cutillas, N.; Vicente, C.; Villa, M. D.; Aviles, F. X.; Lopez, G.; Moreno, V.; Perez, J.; Bautista, D. Palladium(II) and Platinum(II) Organometallic Complexes with the Model Nucleobase Anions of Thymine, Uracil, and Cytosine: Antitumor Activity and Interactions with DNA of the Platinum Compounds. *Inorg. Chem.* **2006**, *45*, 6347–6360. (f) Ruiz, J.; Cutillas, N.; Vicente, C.; Villa, M. D.; Lopez, G.; Lorenzo, J.; Aviles, F. X.; Moreno, V.; Bautista, D. New Palladium(II) and Platinum(II) Complexes with the Model Nucleobase 1-Methylcytosine: Antitumor Activity and Interactions with DNA. *Inorg. Chem.* **2005**, *44*, 7365–7376.

(9) (a) Hoseini, S. J.; Mohamadikish, M.; Kamali, K.; Heinemann, F. W.; Rashidi, M. Organoplatinum complexes containing bis(diphenylphosphino)amine as ligand: uncommon case of N−H···I−Pt hydrogen bonding. *Dalton Trans.* **2007**, 1697–1704. and references therein. (b) Puddephatt, R. J. Chemistry of bis(diphenylphosphino)methane. *Chem. Soc. Rev.* **1983**, *12*, 99–127. (c) Jamali, S.; Rashidi, M.; Jennings, M. C.; Puddephatt, R. J. A comparison of binuclear dimethylplatinum(II) complexes with the bridging ligands X(PPh2)2, X=CH_2 or NH. *Dalton Trans.* **2003**, 2313–2317. (d) Nabavizadeh, S. M.; Golbon Haghighi, M.; Esmaeilbeig, A. R.; Raoof, F.; Mandegani, Z.; Jamali, S.; Rashidi, M.; Puddephatt, R. J. Assembly of Symmetrical or Unsymmetrical Cyclometalated Organoplatinum Complexes through a Bridging Diphosphine Ligand. *Organometallics* **2010**, *29* (21), 4893–4899.

(10) Orlowski, R. Z.; Dees, E. C. The role of the ubiquitination-proteasome pathway in breast cancer: applying drugs that affect the ubiquitin-proteasome pathway to the therapy of breast cancer. *Breast Cancer Res.* **2003**, *5*, 1–7.

(11) Peters, J. M.; Franke, W. W.; Kleinschmidt, J. A. Distinct 19 and 20 S subcomplexes of the 26 S proteasome and their distribution in the nucleus and the cytoplasm. *J. Biol. Chem.* **1994**, *269*, 7709–7718.

(12) Goldberg, A. L. Functions of the proteasome: the lysis at the end of the tunnel. *Science* **1995**, *268*, 522–523.

(13) Dou, Q. P.; Li, B. Proteasome inhibitors as potential novel anticancer agents. *Drug Resist. Updates* **1999**, *2*, 215–223.

(14) Hochstrasser, M. Ubiquitin, proteasomes, and the regulation of intracellular protein degradation. *Curr. Opin. Cell Biol.* **1995**, *7*, 215–223.

(15) Rajkumar, S. V.; Richardson, P. G.; Hideshima, T.; Anderson, K. C. Proteasome Inhibition As a Novel Therapeutic Target in Human Cancer. *J. Clin. Oncol.* **2005**, *23*, 630–639.

(16) Lopes, U. G.; Erhardt, P.; Yao, R.; Cooper, G. M. p53-Dependent Induction of Apoptosis by Proteasome Inhibitors. *J. Biol. Chem.* **1997**, *272*, 12893–12896.

(17) Kane, R. C.; Farrell, A. T.; Sridhara, R.; Pazdur, R. United States Food and Drug Administration Approval Summary: Bortezomib for the Treatment of Progressive Multiple Myeloma after One Prior Therapy. *Clin. Cancer Res.* **2006**, *12*, 2955–2960.

(18) Dou, Q. P.; Goldfarb, R. H. Bortezomib—Millennium Pharmaceuticals. *IDrugs* **2002**, *5*, 828–834.

(19) (a) Jia, L.; Jiang, P.; Xu, J.; Hao, Z.; Xu, X.; Chen, L.; Wu, J.; Tang, N.; Wang, Q.; Vittal, J. J. Synthesis, crystal structures, DNA-binding properties, cytotoxic and antioxidation activities of several new ternary copper(II) complexes of *N*,*N*′-(*p*-xylylene)di-alanine acid and 1,10-phenanthroline. *Inorg. Chim. Acta* **2010**, *363*, 855–865. (b) Barton, J. K.; Danishefsky, A. T.; Goldberg, J. M. Tris(phenanthroline)ruthenium(II): stereoselectivity in binding to DNA. *J. Am. Chem. Soc.* **1984**, *106*, 2172–2176. (c) Kelly, J. M.; Murphy, M. J.; McConell, D. J.; OhUigin, C. A comparative study of the interaction of 5,10,15,20-tetrakis (*N*-methylpyridinium-4-yl)porphyrin and its zinc complex with DNA using fluorescence spectroscopy and topoisomerisation. *Nucleic Acids Res.* **1985**, *13*, 167–184. (d) Hartmann, M.; Robert, A.; Duarte, V.; Keppler, B. K.; Meunier, B. Synthesis of water-soluble ruthenium porphyrins as DNA cleavers and potential cytotoxic agents. *J. Biol. Inorg. Chem.* **1997**, *2*, 427–432. (e) Rajski, S. R.; Williams, R. M. DNA Cross-Linking Agents as Antitumor Drugs. *Chem. Rev.* **1998**, *98*, 2723–2795. (f) Keck, M. V.; Lippard, S. J. Unwinding of supercoiled DNA by platinum-ethidium and related complexes. *J. Am. Chem. Soc.* **1992**, *114*, 3386–3390.

(20) (a) Vandiver, M. S.; Bridges, E. P.; Koon, R. L.; Kinnaird, A. N.; Glaeser, J. W.; Campbell, J. F.; Priedemann, C. J.; Rosenblatt, W. T.; Herbert, B. J.; Wheeler, S. K.; Wheeler, J. F.; Kane-Maguire, N. A. P. Effect of Ancillary Ligands on the DNA Interaction of $[Cr(diimine)_3]^{3+}$ Complexes Containing the Intercalating Dipyridophenazine Ligand. *Inorg. Chem.* **2010**, *49*, 839–848. (b) Tan, J.; Wang, B.; Zhu, L. DNA binding, cytotoxicity, apoptotic inducing activity, and molecular modeling study of quercetin zinc(II) complex. *Bioorg. Med. Chem.* **2009**, *17*, 614–620.

(21) Girolami, G. S.; Rauchfuss, T. B.; Angelici, R. J. *Synthesis and Technique in Inorganic Chemistry*; University Science Books, Sausalito, CA, 1999; p 254.

(22) Milacic, V.; Chen, D.; Ronconi, L.; Landis-Piwowar, K. R.; Fregona, D.; Dou., Q. P. A Novel Anticancer Gold(III) Dithiocarbamate Compound Inhibits the Activity of a Purified 20S Proteasome and 26S Proteasome in Human Breast Cancer Cell Cultures and Xenografts. *Cancer Res.* **2006**, *66*, 10478–10486.

(23) Milacic, V.; Chen, D.; Giovagnini, L.; Diez, A.; Fregona, D.; Dou., Q. P. Pyrrolidine dithiocarbamate-zinc(II) and -copper(II)

complexes induce apoptosis in tumor cells by inhibiting the proteasomal activity. *Toxicol. Appl. Pharmacol.* **2008**, *231*, 24–33.

(24) Chen, D.; Frezza, M.; Shakya, R.; Cui, Q. C.; Milacic, V.; Verani, C. N.; Dou., Q. P. Inhibition of the Proteasome Activity by Gallium(III) Complexes Contributes to Their Anti-Prostate Tumor Effects. *Cancer Res.* **2007**, *67*, 9258–9265.

(25) An, B.; Goldfarb, R. H.; Simian, R.; Dou., Q. P. Novel dipeptidyl proteasome inhibitors overcome Bcl-2 protective function and selectively accumulate the cyclin-dependent kinase inhibitor p27 and induce apoptosis in transformed, but not normal, human fibroblasts. *Cell Death Differ.* **1998**, *5*, 1062–1075.

(26) (a) Song, M. Y.; Wu, Q.; Yang, P. J.; Luan, N. N.; Wang, L. F.; Liu, Y. M. DNA Binding and cleavage activity of Ni(II) complex with all-trans retinoic acid. *J. Inorg. Biochem.* **2006**, *100*, 1685–1691. (b) Wang, B. D.; Yang, Z. Y.; Crewdson, P.; Wang, D. Q. Synthesis, crystal structure and DNA-binding studies of the Ln(III) complex with 6-hydroxychromone-3-carbaldehyde benzoyl hydrazone. *J. Inorg. Biochem.* **2007**, *101*, 1492–1504.

(27) (a) Indumathy, R.; Radhika, S.; Kanthimathi, M.; Weyhermuller, T.; Nair, B. U. Cobalt complexes of terpyridine ligand: Crystal structure and photocleavage of DNA. *J. Inorg. Biochem.* **2007**, *101*, 434–443. (b) Asadi, M.; Safaei, E.; Ranjbar, B.; Hasani, L. Thermodynamic and spectroscopic study on the binding of cationic Zn(II) and Co(II) tetrapyridinoporphyrazines to calf thymus DNA: the role of the central metal in binding parameters. *New J .Chem.* **2004**, *28*, 1227–1234.

(28) Han, G. Y.; Yang, P. Synthesis and characterization of water-insoluble and water-soluble dibutyltin(IV) porphinate complexes based on the tris(pyridinyl)porphyrin moiety, their anti-tumor activity in vitro and interaction with DNA. *J. Inorg. Biochem.* **2002**, *91*, 230–236.

(29) Mansuri-Torshizi, H.; Mital, R.; Srivastava, T. S.; Parekh, H.; Chitnis, M. P. Synthesis, characterization, and cytotoxic studies of α-diimine/1,2-diamine platinum(II) and palladium(II) complexes of selenite and tellurite and binding of some of these complexes to DNA. *J. Inorg. Biochem.* **1991**, *44*, 239–247.

(30) Esmaeilbeig, A.; Samouei, H.; Abedanzadeh, S.; Amirghofran, Z. Synthesis, Characterization and Antitumor Activity Study of Some Cyclometalated Organoplatinum(II) Complexes Containing Aromatic N-Donor Ligands. *J. Organomet. Chem.* **2011**, DOI: 10.1016/j.jorganchem.2011.06.010.

(31) Daniel, K. G.; Chen, D.; Orlu, S.; Cui, Q. C.; Miller, F. R.; Dou., Q. P. Clioquinol and pyrrolidine dithiocarbamate complex with copper to form proteasome inhibitors and apoptosis inducers in human breast cancer cells. *Breast Cancer Res.* **2005**, *7*, R897–908.

(32) Zsila, F.; Bikadi, D. Z.; Simonyi, M. Circular dichroism spectroscopic studies reveal pH dependent binding of curcumin in the minor groove of natural and synthetic nucleic acids. *Org. Biomol. Chem.* **2004**, *2*, 2902–2910.

(33) Marmur, J. A procedure for the isolation of deoxyribonucleic acid from micro-organisms. *J. Mol. Biol.* **1961**, *3*, 208–218.

(34) Philip, K. W.; Malkhaz, K.; Qu, Y.; Nicholas, F. A circular dichroism study of ethidium bromide binding to Z-DNA induced by dinuclear platinum complexes. *J. Inorg. Biochem.* **1996**, *63*, 9–18.

(35) (a) De Pascali, S. A.; Migoni, D.; Papadia, P.; Muscella, A.; Marsigliante, S.; Ciccarese, A.; Fanizzi, F. P. New water-soluble platinum(II) phenanthroline complexes tested as cisplatin analogues: first-time comparison of cytotoxic activity between analogous four- and five-coordinate species. *Dalton Trans.* **2006**, 5077–5087. (b) Bigioni, M.; Ganis, P.; Panunzi, A.; Ruffo, F.; Salvatore, C.; Vito, A. Electrophilic Attack of $[I(py)_2]^+(NO_3^-)$ on Three-Coordinate Pt^0 Precursors: Synthesis and In Vitro Antitumor Activity of Water-Soluble, Five-Coordinate Pt^{II} Complexes. *Eur. J. Inorg. Chem.* **2000**, 1717–1721. (c) Garciìa-Seijo, M. I.; Habtemariam, A.; Del Socorro Murdoch, P.; Gould, R. O.; García-Fernández, M. E. Five-coordinate aminophosphine platinum(II) complexes containing cysteine derivatives as ligands. *Inorg. Chim. Acta* **2002**, *335*, 52–60.